INTERFACE SCIENCE 9, 357–363, 2001

Grain Boundary Motion during Ag and Cu Grain Boundary Diffusion in Cu Polycrystals

S.V. DIVINSKI, M. LOHMANN, T. SURHOLT AND CHR. HERZIG
Institut für Materialphysik, Universität Münster, Wilhelm-Klemm-Str. 10, D-48149 Münster, Germany

Abstract. Grain boundary (GB) motion in high-purity Cu material (5N8 and 5N Cu) is investigated using the results of radiotracer GB diffusion measurements with tracers exhibiting fundamental differences in the solute-matrix atom interactions. The results on GB solute diffusion of Ag (revealing a miscibility gap in the Ag-Cu phase diagram) and Au (forming intermetallic compounds with Cu) in Cu and on Cu self-diffusion are analyzed.

The initial parts of the Ag and Cu penetration profiles turned out to be substantially curved. The profile curvature is explained via the effect of GB motion during ^{110m}Ag and ^{64}Cu GB penetration. The activation enthalpies of GB motion in these two independent measurements occurred to be very close, 95 and 103 kJ/mol, respectively. Moreover, these values turn out to be close, but still somewhat larger than the activation enthalpy of Cu GB self-diffusion in Cu material of the same very high purity, $Q_{\mathrm{gb}}^{\mathrm{Cu}} = 72$ kJ/mol. Although tracer diffusion measurements of Au GB diffusion in Cu yielded only limited information on GB motion, the absolute values of GB velocities are consistent with those calculated from the Ag and Cu GB diffusion data.

Keywords: Cu, grain boundary diffusion, grain boundary segregation, grain boundary motion

1. Introduction

Grain boundary (GB) migration is involved in a number of diffusion-controlled processes, such as dissolution and coarsening, discontinuous precipitations, and recrystallization (for a review see e.g. [1]). In addition, the diffusing solute can itself induce migration of grain boundaries, e.g. during Diffusion-Induced Grain boundary Migration (DIGM) [2] or Diffusion-Induced Recrystallization (DIR) [3] processes. According to a conventional picture of interface migration [4], the migration occurs by atoms leaving the grain on one side of the interface (parent grain), diffusing through the interface, and by subsequent deposition on the other side of the interface. Therefore, GB diffusion of matrix and impurity atoms *across the interface* plays an important role in these processes.

In typical grain boundary diffusion experiments the tracer diffusivity *along the interfaces* is measured. Experimental findings indicate that the diffusion barriers are essentially the same for diffusion along and across GBs [5] and this circumstance allowed the elaboration of consistent theory to process the GB diffusion penetration profiles in polycrystals when part of the grain boundaries moves during the diffusion anneal [5, 6]. Such a treatment presents a unique opportunity to study the GB motion in high-purity materials, since GB diffusion measurements by the radiotracer method are generally very sensitive and can be carried out on polycrystals at very low tracer concentrations.

In the present work the GB motion in the same high-purity Cu material (5N8 Cu) is investigated using the results of radiotracer GB diffusion measurements conducted with different tracers exhibiting fundamental differences in the solute-matrix atom interactions. GB solute diffusion of Ag (revealing a miscibility gap in the Ag-Cu phase diagram) and Au (forming intermetallic compounds with Cu) in Cu will be analyzed as well as Cu GB self-diffusion in the same material. This will allow us to discuss the predicted effect of chemical interactions between tracer and matrix atoms on GB motion in the limit of small GB velocities [7]. The grain boundary diffusion along stationary boundaries in this Cu material was thoroughly

Table 1. The parameters of Ag GB diffusion in the 5N8 Cu material [8]. T, t, and D_v are the temperature, time, and bulk diffusivity, respectively. The parameters q_3, q_4, q_5, and q_6 were determined by the least-square fit according to Eq. (1).

T (K)	t (s)	D_v (m^2s^{-1})	q_5/q_3	q_4 (10^4 m^{-1})	q_6 (10^5 $m^{-6/5}$)	V ($m\,s^{-1}$)	γ
923	77000	6.0×10^{-16}	0.33	8.0 ± 1.3	5.25 ± 0.12	$(5.3 \pm 0.3) \times 10^{-10}$	6
826	66000	3.1×10^{-17}	0.40	6.4 ± 0.8	3.60 ± 0.2	$(2.3 \pm 0.6) \times 10^{-10}$	11
723	93700	5.4×10^{-19}	0.40	5.0 ± 1.8	2.63 ± 0.04	$(3.4 \pm 2.0) \times 10^{-11}$	14
675	279000	5.4×10^{-20}	0.19	3.54 ± 0.08	1.81 ± 0.04	$(7.4 \pm 0.1) \times 10^{-12}$	17
623	260000	3.0×10^{-21}	0.58	3.91 ± 0.08	1.62 ± 0.02	$(2.1 \pm 0.1) \times 10^{-12}$	20

discussed for Ag [8], Au [9], and Cu [10] GB diffusion.

2. Experimental Procedure

Copper with nominal purities 5N8 (Ag and Cu GB diffusion) and 5N (Au GB diffusion) was used. The impurity content of the materials with respect to some selected impurities is given in Table 1 in Ref. [10]. The main difference between both materials is the content of sulfur which amounts to 0.1 ppm in 5N8 and 1 ppm in 5N Cu [10]. After cold deformation of the ingots, resulting in reduction of the grain size, the bars were sealed into quartz tubes and annealled in two steps: first at 523 K for 4 days (stress relaxation) and then at 1023 K for 24 hours (recrystallization). The average grain size was measured to be about 60 to 80 μm. The samples of about 3 mm in thickness, which were subsequently cut from the bars, were sealed in quartz tubes and subjected to the pre-diffusion anneal at the temperature and for at least the time of the intended diffusion anneal to ensure quasi-equilibrium conditions for the GB segregation of all residual impurity elements.

The radiotracer ^{110m}Ag was used in form of nitrate solution and deposited on the sample by evaporation in a high-vacuum chamber. The radiotracer ^{64}Cu was produced by exposing copper with natural isotope composition to neutron irradiation at the reactor of the GKSS Forschungszentrum (Geesthacht, Germany), dissolved in dilute nitric acid, and dropped onto the sample surface. Finally, the carrier-free radioisotope ^{195}Au was used in the form of an HCl solution. The samples were sealed in quartz tubes in a purified (5N) Ar atmosphere and subjected to the given diffusion anneals within the temperature interval from 623 to 980 K. The temperatures were measured and controlled with Ni-NiCr thermocouples with an accuracy of about ± 1 K. After the diffusion anneal the samples were reduced in diameter (at least 1 to 2 mm) to remove the effect of lateral-surface diffusion. The penetration profiles were determined by the sectioning technique. The activity of each section was determined by measuring the intensity of the β radiation of the ^{110m}Ag and ^{64}Cu tracer in a liquid-scintillation counter and in a well-type intrinsic Ge γ detector for the ^{195}Au tracer.

3. Results

Typical penetration profiles measured for ^{110m}Ag, ^{64}Cu, and ^{195}Au GB diffusion are shown in Fig. 1(a)–(c), respectively. These measurements were carried out in the so-called B type diffusion regime, when the tracer atom distribution at sufficiently large depths is governed by short-circuit diffusion along GBs and simultaneous out-diffusion from the grain boundaries to the grain interior through bulk diffusion [11]. The bulk diffusion length extends to about several micrometers which is notably smaller than the grain size in these experiments (about 60 to 80 μm). Under such conditions, according to theoretical arguments [12], the GB diffusion profiles should be linear in coordinates $\ln \bar{c}$ vs. $y^{6/5}$, where $\bar{c}$ is the layer concentration and y the penetration depth. This behavior is indeed observed at depths larger than 100–150 μm (Fig. 1).

However, at the depths 10 $\mu\text{m} \le y \le 70$ μm the present profiles deviate from the ideal form which is represented by a surperposition of direct volume diffusion and short-circuit diffusion along GBs, dashed lines in Fig. 1(a)–(c). In [8] it was clearly demonstrated that such curvature of Ag penetration profiles cannot be attributed to a possible non-linear segregation behavior of Ag at Cu GBs, since the *absolute* concentrations of the tracer atoms in GBs were proved to be very small in these experiments (lower than 10^{-4} atomic fractions at $y > 10$ μm) and fall well into the dilute limits of GB segregation. Similar arguments also hold for Au diffusion in Cu GBs, since the carrier-free ^{195}Au

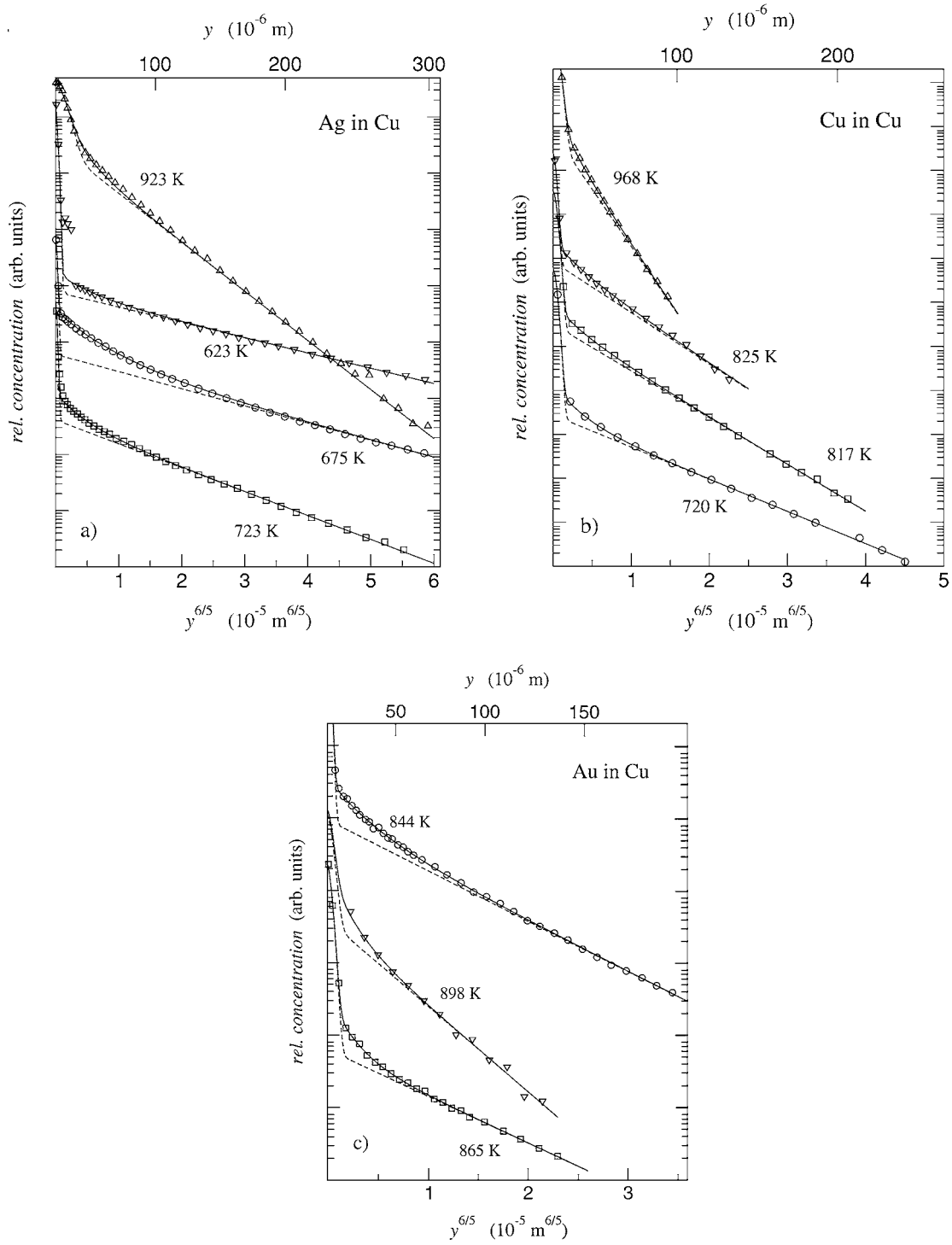

Figure 1. Typical penetration profiles of Ag (a), Cu (b), and Au (c) GB diffusion in Cu. The results of the fits accounting for bulk plus GB diffusion over stationary boundaries (dashed lines) and for bulk plus GB diffusion over both moving and stationary boundaries (solid lines) are shown.

radioisotope was used. Therefore, a different reason has to be responsible for the observed shape of the profiles.

4. Penetration Profiles in the Presence of Stationary and Moving Boundaries

To explain the form of our experimental profiles GB migration during the diffusion anneal has to be taken into account. In the present work a careful pre-diffusion heat treatment has been applied to approach thermodynamic equilibrium with respect to the GB segregation of impurity atoms, which should simultaneously decrease a possible migration of the GBs during the diffusion anneal. However, since very pure Cu material was used, it was impossible to suppress the GB migration totally.

It is known that if a certain fraction f of the GBs moves during the diffusion experiment, the concentration profiles are modified and their treatment depends on the given kinetic regime [5]. To analyse the diffusion profiles, a simplifying assumption is adopted that the migrating boundaries move with the same constant velocity V during the time t of the diffusion experiment. It is additionally assumed that the grain boundary migration distance Vt and the volume diffusion length $\sqrt{D_v t}$ remain smaller than the average grain size d [5] (D_v is the bulk diffusion coefficient). The subsequent treatment will demonstrate that these assumptions are appropriate for our experiments. If the parameter γ, determined as $\gamma = \frac{Vt}{\sqrt{D_v t}}$, is sufficiently large, namely if $\gamma > 6$ [5], the diffusion process becomes steady-state and the concentration profiles should approximately be presented as a sum of three exponents (for the thin-layer initial conditions under the B-regime kinetics)

$$\bar{c} \cong q_1 \exp(-q_2 y^2) + q_3 \exp(-q_4 y) + q_5 \exp(-q_6 y^{6/5}) \tag{1}$$

with six fitting parameters $q_1, \ldots, q_6$. From the form of Eq. (1) it is seen that q_1 and q_2 describe the direct bulk diffusion process (usually dislocation-enhanced, especially at the lowest temperatures); q_5 and q_6 correspond to diffusion along stationary GBs under the B regime conditions; and q_3 and q_4 stem from the contribution of moving boundaries. Thus, performing the fit according to Eq. (1) and assuming that the diffusivities of stationary and moving boundaries are nearly the same the GB velocity V can be estimated as [5]

$$V = P \cdot q_4^2. \tag{2}$$

Here $P = s \cdot \delta \cdot D_{\mathrm{gb}}$ is the triple product which determines diffusivity along stationary GBs (s is the segregation coefficient, δ the GB width, and D_{gb} the GB diffusion coefficient) and which is evaluated via a standard expression [12]

$$P = 1.308 \sqrt{\frac{D_v}{t}} q_6^{-5/3}. \tag{3}$$

Note that formally D_v may be determined from the value of q_2 as $D_v = 1/(4q_2 t)$. However, the experimental error of such a determination of the bulk diffusion coefficient would be very large, since the present experiments were not devoted to measure bulk diffusion and only a few representative points of the profiles are available at relevant depths, see Fig. 1(a)–(c). Therefore, the data of direct measurements of Ag bulk diffusion in Cu [13], Cu self-diffusion in Cu [14], and Au diffusion in Cu [15] were used in the present work:

$$D_v^{\mathrm{Ag}} = 6.1 \times 10^{-5} \cdot \exp\left(-\frac{194.4\ \mathrm{kJ \cdot mol^{-1}}}{RT}\right) \mathrm{m^2 s^{-1}}, \tag{4}$$

$$D_v^{\mathrm{Cu}} = 1.0 \times 10^{-5} \cdot \exp\left(-\frac{198.8\ \mathrm{kJ \cdot mol^{-1}}}{RT}\right) \mathrm{m^2 s^{-1}}, \tag{5}$$

$$D_v^{\mathrm{Au}} = 0.8 \times 10^{-5} \cdot \exp\left(-\frac{191.0\ \mathrm{kJ \cdot mol^{-1}}}{RT}\right) \mathrm{m^2 s^{-1}}. \tag{6}$$

Since as many as six fitting parameters are involved in Eq. (1), the results may appreciably depend on the given fitting procedure. The following procedure was applied by us to obtain the most reliable results. At first, the parameters q_5 and q_6 were determined from the fit of the linear tails of the experimental profiles in coordinates $\ln \bar{c}$ vs. $y^{6/5}$. As a next step, the near surface experimental points were used to determine the parameter q_2. Then all experimental points were included in the fit according to Eq. (1) to establish the values q_1, q_3, and q_4 keeping q_2, q_5, and q_6 constant. Finally, these data of $q_1, \ldots, q_6$ were used as start values in the main fit including all experimental points and all unknown parameters q_i. The results are given in Tables 1–3, where the values q_6, q_5/q_3, and q_4, which are relevant for the subsequent treatment, are presented. The value of q_6 is connected by an obvious relation, see Eq. (3), to the value of the triple product P. The quality of our fit is presented in Fig. 1(a)–(c) (solid

Table 2. The parameters of Cu GB self-diffusion in Cu materials of the 5N8 and 5N purities [10]. The parameters q_3, q_4, q_5, and q_6 were determined by the profile fit according to Eq. (1).

T (K)	q_5/q_3	q_4 (10^4 m^{-1})	q_6 (10^5 m$^{-6/5}$)	V (m s^{-1})	γ
5N8 Cu					
968	0.20	14.9 ± 1.3	5.97 ± 0.12	$(9.2 \pm 0.8) \times 10^{-10}$	6
872	0.31	10.2 ± 1.3	3.16 ± 0.12	$(1.9 \pm 0.7) \times 10^{-10}$	8
825	0.26	7.51 ± 0.8	2.76 ± 0.20	$(5.7 \pm 2.2) \times 10^{-11}$	6
817	0.43	7.42 ± 1.8	2.45 ± 0.04	$(5.4 \pm 1.2) \times 10^{-11}$	7
740	0.66	6.64 ± 0.1	1.99 ± 0.04	$(1.2 \pm 0.6) \times 10^{-11}$	8
720	0.20	7.58 ± 0.1	1.68 ± 0.02	$(1.2 \pm 0.4) \times 10^{-11}$	16
5N Cu					
923	0.44	14.7 ± 2.1	2.15 ± 0.05	$(4.2 \pm 0.6) \times 10^{-10}$	5
877	0.60	9.70 ± 3.5	4.76 ± 0.08	$(1.0 \pm 0.6) \times 10^{-10}$	4

Table 3. The parameters of Au GB self-diffusion in the 5N Cu material [9]. The parameters q_3, q_4, q_5, and q_6 were determined by the profile fit according to Eq. (1).

T (K)	q_5/q_3	q_4 (10^4 m^{-1})	q_6 (10^5 m$^{-6/5}$)	V (m s^{-1})	γ
898	0.17	11.4 ± 7.3	2.73 ± 0.22	$(7.5 \pm 3.1) \times 10^{-10}$	13
865	0.17	9.0 ± 1.1	1.48 ± 0.05	$(2.3 \pm 0.7) \times 10^{-10}$	24
844	0.31	6.2 ± 0.7	1.60 ± 0.06	$(1.0 \pm 0.3) \times 10^{-10}$	8
739	0.40	8.0 ± 4.8	0.89 ± 0.12	$(1.9 \pm 1.5) \times 10^{-11}$	42
666	0.41	10.1 ± 2.0	0.83 ± 0.04	$(9.3 \pm 0.7) \times 10^{-12}$	50

lines). Two types of fitting curves are presented: with (soild lines) and without (dashed lines) accounting for the GB migration (in other words, with q_3 listed in Tables 1–3 and with $q_3 = 0$). It is seen that the model fit by Eq. (1) corresponds well to the experimental profiles. This presentation clearly demonstrates the effect of moving boundaries. The condition $\gamma > 6$ used in the derivation of Eqs. (1) and (2) can be verified from Tables 1–3.

Assuming that the driving force F for the grain boundary migration is roughly the same in all cases, the activation enthalpy Q_m of GB migration was estimated from the plot of VT against $1/T$ using the relation $V \propto \frac{D_\mathrm{m}}{RT} F$ [5]. Here D_m is the coefficient of atomic diffusion *across* the grain boundary, which is commonly accepted to be responsible for the grain boundary motion. The relevant plots are presented in Fig. 2. The following Arrhenius relations for boundary motion during the diffusion anneals were derived from the measurements of Ag and Cu GB diffusion in the same

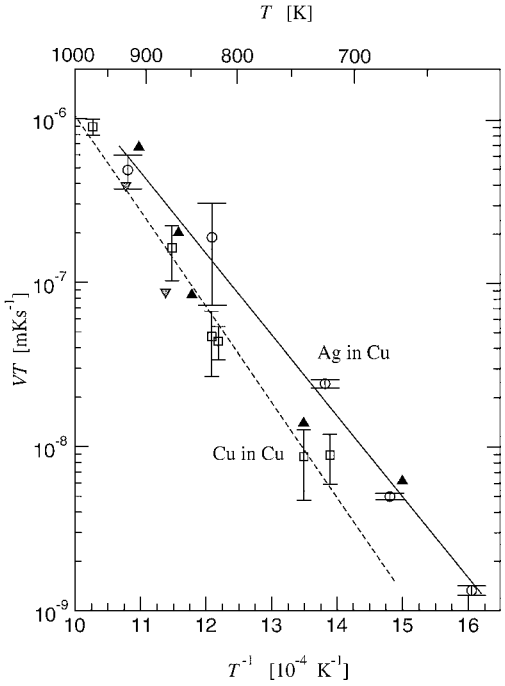

Figure 2. The product VT (velocity times temperature) determined from the GB diffusion data for Ag in 5N8 Cu (circles), Cu in 5N8 Cu (squares), Cu in 5N Cu (triangles down), and Au in 5N Cu (triangles up) as function of the inverse temperature.

5N8 Cu material:

$$VT^{(\mathrm{Ag})} = \left(0.2^{+0.3}_{-0.1}\right) \exp\left\{-\frac{(95 \pm 10)\ \mathrm{kJ \cdot mol^{-1}}}{RT}\right\} \mathrm{mKs^{-1}} \tag{7}$$

and

$$VT^{(\mathrm{Cu})} = \left(0.7^{+1.7}_{-0.5}\right) \exp\left\{-\frac{(103 \pm 12)\ \mathrm{kJ \cdot mol^{-1}}}{RT}\right\} \mathrm{mKs^{-1}}, \tag{8}$$

respectively. Corresponding lines are drawn in Fig. 2 for comparison. The experiments on Au GB diffusion in the 5N Cu material yielded the following Arrhenius parameters for the GB mobility:

$$VT^{(\mathrm{Au})} = \left(0.1^{+1.1}_{-0.09}\right) \exp\left\{-\frac{(94 \pm 17)\ \mathrm{kJ \cdot mol^{-1}}}{RT}\right\} \mathrm{mKs^{-1}}. \tag{9}$$

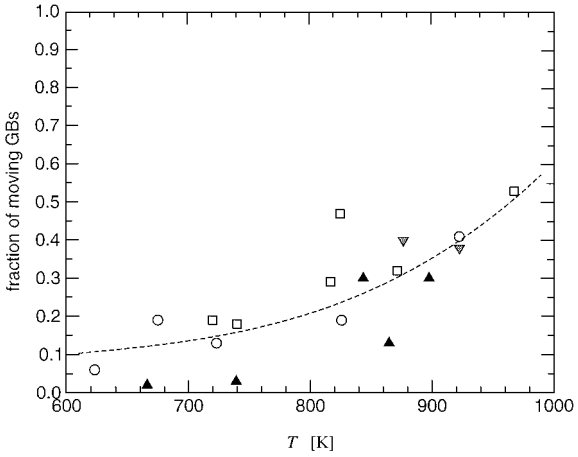

Figure 3. The fraction of moving boundaries as function of temperature T for various data sets: Ag GB diffusion in 5N8 Cu (circles), Cu GB self-diffusion in 5N8 Cu (squares) and in 5N Cu (triangles down), and Au GB diffusion in 5N Cu (triangles up). The dashed line is drawn as a guidance for eyes.

These values of the grain boundary mobility (triangles up in Fig. 2) are in general agreement with the two other data sets.

The fraction f of moving boundaries can be evaluated as [5]

$$f = \frac{1}{1 + 0.3205 \cdot \left(\frac{q_5}{q_3}\right)\gamma^{3/2}}. \qquad (10)$$

The results of different measurements are summarized in Fig. 3 and it is seen that f generally increases with increasing temperature, as it can be expected. However, the exact values of f should be treated with caution due to large errors incorporated in the fitting procedure of Eq. (1) and due to the rough model approximations used to analyse the contribution of moving boundaries (see below).

5. Discussion and Conclusions

In [10] Cu GB self-diffusion was measured in two different Cu materials with the nominal 5N and 5N8 purities. The GB self-diffusivity in the 5N8 Cu material was found to be systematically larger and the activation enthalpy ($Q_{\mathrm{sd}}^{(5N8)} = 72$ kJ/mol) lower than for Cu GB self-diffusion in 5N copper ($Q_{\mathrm{sd}}^{(5N)} = 86$ kJ/mol), revealing the effect of strongly segregating residual impurities (e.g. S in Cu) [10]. It was therefore interesting to compare the GB mobilities in these two high-purity materials. Processing the penetration profiles in [10], the GB motion effect in the 5N Cu material can reliably be detected only at a few temperatures. The results are also summarized in Table 2. The velocities of GB motion in both copper materials turned out to be quite similar, as seen by comparing the squares (5N8 Cu) and inverted triangles (5N Cu) in Fig. 2. This result can be understood by the fact that mainly the fastest GBs affect the penetration profiles and these are the "cleanest" boundaries. The slower boundaries appear as being effectively immobile during the diffusion anneal and their contribution is superimposed to that of stationary boundaries.

Figure 2 summarizes the results of the different data sets. As a main result, a general consistency between the different, independent measurements is seen. Obviously the average GB velocity does not depend on the given tracer type. The applied tracer atoms thus serve as a "probe" to detect the GB motion, but do not initiate and/or affect it substantially in the present experiments.

The concentration of tracer atoms is small enough to correspond to the dilute limit at the depths where the contribution of the moving GBs dominates. In [7], the effect of impurity segregation on GB motion was analyzed accounting for their possible non-linear segregation. It was concluded that at small average GB velocities (which is also our case) the segregation of those solutes, which are immiscible in the matrix (e.g. Ag in Cu), should result in a slight increase of GB velocities and in a decrease of the activation enthalpy of the GB motion. On the other hand, it was argued that solutes forming intermetallic compounds with the matrix atoms (e.g. Au in Cu) should substantially suppress the GB mobility and the activation enthalpy of GB motion should be notably increased [7]. Such an effect is not observed at the temperatures of the present investigations, supporting the idea that in our conditions the tracers do not disturb the observed GB motion in Cu.

The general agreement of all data sets (Fig. 2) confirms the validity of the approach suggested in [5, 6] despite a number of simplifying assumptions adopted in the model. In real polycrystals there exists a continuous spectrum of GB velocities and their directions. Moreover, GBs often reveal a jerky (stop-and-go) motion. The value of the GB velocity determined in the adopted scheme is averaged over the fastest GBs which predominantly contribute to the profile curvature and presents a well-difined value for a given polycrystalline material. Otherwise it would be difficult to explain such

good correspondence among the independent measurements on the same material.

The fraction f of moving GBs increases with increasing temperature, as it should be expect, Fig. 3. Moreover, a tendency is seen that f in less pure Cu material (5N Cu, solid symbols in Fig. 3) becomes somewhat lower than f in 5N8 Cu material (open symbols in Fig. 3) with decreasing temperature at $T < 800$ K. This fact can be understood in terms of an increasing tendency of residual impurities to segregate at GBs, to build impurity atmospheres around them, and to decrease their mobility due to the "impurity drag" effect [17, 18]. Nevertheless, the fastest GBs have similar velocities in both materials, see Fig. 2.

The calculated values of the GB migration from the data sets for Cu, and Au GB diffusion in Cu, $Q_m = (95 \pm 10)$, (103 ± 12), and (94 ± 17), Ag, kJ·mol^{-1} respectively, are somewhat larger than the activation enthalpy Q_{sd} of the GB self-diffusion in the 5N8 Cu material, $Q_{sd} = (72.5 \pm 1.5)$ kJ·mol^{-1} [10], and remain larger than the same value for GB self-diffusion in 5N Cu, $Q_{sd} = (84.8 \pm 2.8)$ kJ·mol^{-1} [10]. A similar value of the activation enthalpy of Cu GB self-diffusion was measured in the nominal 6N Cu material, $Q_{sd} = 80.9$ kJ·mol^{-1} by Gupta [19] (cf. comments on these results in Ref. [10]. Nevertheless this difference in activation enthalpies may be considered as acceptable in view of the errors incorporated in the fitting procedure according to Eq. (1).

References

1. G. Gottstein and L.S. Shvindlerman, *Grain Boundary Migration in Metals: Thermodynamics, Kinetics, Applications* (CRC Press, Boca Raton, FL, 1999).
2. D.B. Butrymowicz, D.E. Newbury, D. Turnbull, and J.W. Cahn, Scripta Metall. **18**, 1005 (1984).
3. F.J.A. den Broeder and S. Nakahara, Scripta Metall. **17**, 399 (1983).
4. M. Hillert, Acta Mater. **47**, 4481 (1991).
5. F. Güthoff, Y. Mishin, and Chr. Herzig, Z. Metallkd. **84**, 584 (1993).
6. Y. Mishin and I.M. Razumovskii, Acta Metall. Mater. **40**, 597 (1992).
7. M.I. Mendelev and D.J. Srolovitz, Acta Mater. **48**, 589 (2001).
8. S.V. Divinski, M. Lohmann, and Chr. Herzig, Acta Mater. **49**, 249 (2001).
9. T. Surholt, Y. Mishin, and Chr. Herzig, Phys. Rev. B **50**, 3577 (1994).
10. T. Surholt and Chr. Herzig, Acta Metall. **45**, 3817 (1997).
11. L.G. Harrison, Trans. Faraday Soc. **57**, 597 (1961).
12. T. Suzuoka, J. Phys. Soc. Japan **19**, 839 (1964).
13. G. Barreau, G. Brunel, G. Cizeron, and P. Lacombe, C.R. Acad. Sci. (Paris) C **270**, 516 (1970).
14. K. Maier, Phys. Stat. Sol. B **44**, 567 (1977).
15. S. Fujikawa, M. Werner, H. Mehrer, and A. Seeger, in *Vacancies and Interstitials in Metals and Alloys*, Vols. 15–18 of Materials Science Forum, edited by C. Abromeit and H. Wollenberger (Trans Tech, Aedermannsdorf, 1987), p. 431.
16. M. Köppers, Y. Mishin, and Chr. Herzig, Acta Metall. Mater. **42**, 2859 (1994).
17. K. Lücke and K. Detert, Acta Metal. **5**, 628 (1957).
18. J.W. Cahn, Acta Metall. **10**, 789 (1962).
19. D. Gupta, Mater. Re. Soc. Symp. Proc. **337**, 209 (1994).